c0060 # Architected adhesive joints with improved fracture toughness

34

Thomas Pardoen[a], *Kevin T. Turner*[b], *and Michal K. Budzik*[c]
[a]Institute of Mechanics, Materials and Civil Engineering Ecole Polytechnique de Louvain-Louvain School of Engineering, Université Catholique de Louvain, Ottignies-Louvain-la-Neuve, Belgium, [b]Department of Mechanical Engineering and Applied Mechanics, University of Pennsylvania, Philadelphia, PA, United States, [c]Department of Mechanical and Production Engineering, Aarhus University, Aarhus, Denmark

s0010 ## 34.1 Introduction

p0010 Assembly through adhesive bonding of primary and load-carrying components often requires the use of stiff and reliable joining materials with relatively high strength. Such materials often are limited by a relatively low toughness and a high sensitivity to initial flaws and cracks. Thus, much of the focus in the structural adhesive community has been on improving the damage tolerance of bondline materials. This has been achieved through a number of strategies, including reformulating adhesives, as discussed for several adhesive families in Part I, and introducing additional phases or materials (e.g., toughening phases at the nano- and microscales that dissipate energy during failure) as discussed in Chapters 7 and 8.

p0015 On the verge of the green transition, with the focus shifting toward optimized material usage, it is challenging and limiting to focus solely on adhesive chemistry and composition for improvement (e.g., because of the proprietary nature of formulations, long development times, inherent difficulty in realizing continued improvements, etc.). Hence, there is strong motivation to find extrinsic approaches based on structuring and geometry that can be used to toughen adhesive joints and applied to a broad range of materials, independent of chemistry and composition, while possibly also providing an opportunity for lightweighting. The focus of this chapter is on the use of architecture at the scale of tens to a hundred micrometers and above and is distinct from toughening strategies based on nanoscale particles and fibers [1,2]. Such architecture-based approaches have been used to realize bulk mechanical metamaterials (MM) with the goal to realize higher-performance materials, materials with unique combinations of properties, or unconventional properties (e.g., negative Poisson's ratio). The time has come to advance such a paradigm owing to progress in manufacturing, notably digital manufacturing, in the context of adhesive bonding. Contrary to the common paradigm of material continuity and isotropy, some emerging architected materials introduce predetermined defects that allow for extra energy dissipation. These "defects," if correctly designed, can have a beneficial effect by improving toughness without significant loss of stiffness. Note that one of the basic toughening principles is to increase plastic dissipation by designing the joint thickness

Advances in Structural Adhesive Bonding. https://doi.org/10.1016/B978-0-323-91214-3.00012-0

B978-0-323-91214-3.00012-0, 00012

to optimize the plastic zone size. This is the specific subject of Chapter 18, and the underlying principle of increasing plastic dissipation will be further exploited here through variations of this idea. In this chapter, we first review several principles that can be used to enhance toughness and then show several embodiments of these principles through architecting of joints.

s0015 34.2 Overview of working principles for extrinsic joint toughening

s0020 34.2.1 Enhancement through crack deflection

p0020 Consider Fig. 34.1 in which a bonded version of the single edge notched tensile (SENT) specimen is subjected to mode I fracture loading via a remote stress σ^{∞}. If the bondline is of constant thickness t_a, Young's modulus E_a, and fracture energy $\mathcal{G}_{Ic_a}$, and without any flaws or shape variations, a crack growing along a path located in the middle of the adhesive thickness is expected. However, in the illustrated situation, one of the adherends (with Young's modulus E and fracture energy $\mathcal{G}_{Ic} \gg \mathcal{G}_{Ic_a}$) includes a pattern such that the adhesive thickness is locally affected, and the feature intersects the expected crack path. The detailed view of the feature in Fig. 34.1 illustrates the local crack growth scenario expected for this joint configuration. This discussion is simplified and qualitative. The crack propagates toward the feature under mode I loading (denoted as I). Once the tip reaches the feature, continued mode I crack propagation through the feature is energetically unfavorable as $\mathcal{G}_{Ic_a} \ll \mathcal{G}_{Ic}$. Instead, the crack propagates along the vertical edge of the feature. The crack grows along this path under, predominantly, mode II, and mode II generally requires additional energy [3]. Once the vertical edge is bypassed, the crack propagates under mode I either at the

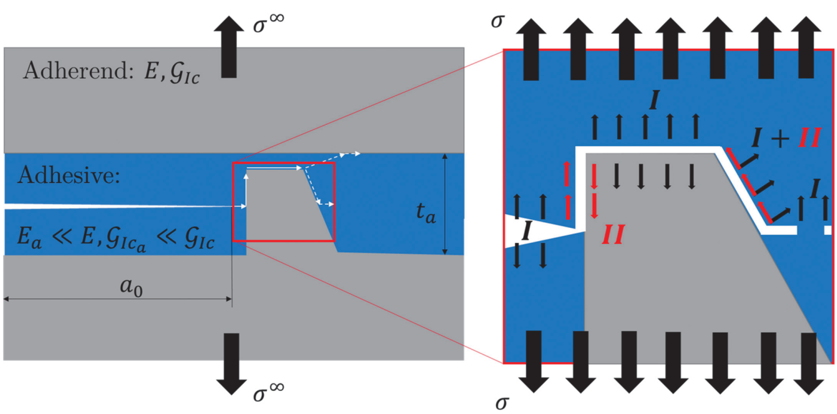

f0010 **Fig. 34.1** Schematic representation of bonded single edge notch test specimen under mode I loading. The feature on one of the adherends deflects the crack from its original path and orientation. On the right, a detailed view of local stress distribution giving rise to different fracture modes.

interface (as in the figure) or cohesively inside the thin adhesive, requiring less energy. The trailing edge of the feature is arbitrarily oriented with respect to the loading direction and a mixed-mode I/II path is expected with intermediate energy expenditure *I/II*, before the mode I cohesive cracking process resumes.

p0025 Though simplified, this example captures the basic idea behind enhancing properties of adhesive joints through crack deflection. Analysis performed using interface fracture mechanics shows that the introduction of mixed-mode conditions leads to a significant increase of the apparent fracture toughness [4]. An entire family of failure criteria exists for determining interface fracture under mixed-mode conditions and crack deflection. The simple linear failure criterion for mixed-mode fracture is given by [5]:

$$\frac{\mathcal{G}_I}{\mathcal{G}_{Ic}} + \frac{\mathcal{G}_{II}}{\mathcal{G}_{IIc}} + \frac{\mathcal{G}_{III}}{\mathcal{G}_{IIIc}} = 1 \tag{34.1}$$

where $\mathcal{G}_I, \mathcal{G}_{II}$, and $\mathcal{G}_{III}$ are the energy-release rates for mode I, II, and III fractures, respectively, and $\mathcal{G}_{Ic}, \mathcal{G}_{IIc}$, and $\mathcal{G}_{IIIc}$ are the respective fracture energies, with a common (although not always respected) inequality $\mathcal{G}_{IIc} > \mathcal{G}_{IIIc} > \mathcal{G}_{Ic}$. Under a globally applied mode I fracture loading, the stresses and, thus, the related magnitudes of $\mathcal{G}_I, \mathcal{G}_{II}$, and $\mathcal{G}_{III}$ are locally set by material heterogeneities and geometric features than can lead to crack deflection and an increase in the apparent fracture toughness. Choosing the ratio of adhesive/feature elastic and fracture properties, along with the shape and position of the crack-deflecting feature, can be used as a tool to control the toughness and crack growth process in general. Designing interfaces to exploit crack deflection is underexplored [6] to the authors' knowledge, though a significant number of works have theoretically investigated crack deflection [3,7,8] and proved the general validity of the concept [9].

s0025 34.2.2 Blunt the propagating crack, relax the stress intensity factor at the tip

p0030 Crack tip blunting is an efficient way to increase the apparent fracture toughness of a material. An elastic material containing a crack of length a under remote tensile loading σ^∞ can be effectively toughened through a straightforward, crack-blunting architecture. Consider an adhesive joint under remote tensile load σ^∞ similar to that previously discussed and depicted in Fig. 34.2A.

p0035 The shape of the crack tip region can be approximated by an ellipse with a major axis a and minor axis b. The maximum stress σ_{max} at the tip can be then expressed as:

$$\sigma_{max} = 2\sigma^\infty \frac{a}{b} \tag{34.2}$$

p0040 As the ratio $\frac{a}{b}$ increases, so does the maximum stress. In the limit of $a \to \infty$ or $b \to 0$, the crack is sharp and linear elastic fracture mechanics (LEFM) applies. Under LEFM, the stress at distance r from the front of the crack tip is (for mode I fracture along the crack growth plane):

B978-0-323-91214-3.00012-0, 00012

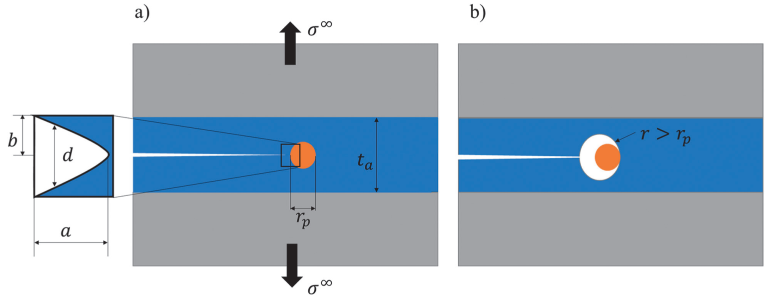

f0015 **Fig. 34.2** Plastic zone radius r_p inside a bondline of thickness t_a under remote tensile stress σ^∞ (A). The local crack tip geometry can be approximated by an ellipse with major a and minor b (zoomed). The introduction of the geometrical feature of radius $r > r_p$ inside the bondline can be used to enhance fracture properties (B).

$$\sigma(r) \approx \frac{K_I}{\sqrt{2\pi r}} \tag{34.3}$$

where K_I is the stress intensity factor, and, in the elastic limit, $K_I^2 \propto E\mathcal{G}_I$. Omitting effects at the atomic scale, many structural adhesives, including untoughened epoxy and polyester-based materials, behave in an apparent elastic-brittle manner. Considering bondlines made of such materials, the internal flaws and microcracks lead to singular stresses at their tips leading to failure at low loads. In addition, while being stiff, the brittle materials do not dissipate significant energy during fracture. In such cases, enabling unloading of the crack tip regions is an efficient solution for improving load capacity.

p0045 Locally at the crack tip, for elastic materials, the intensity/magnitude of the crack tip loading can be reformulated in terms of the crack tip opening displacement (CTOD), defined as:

$$d \sim \frac{K_I^2}{E\sigma_0} \sim \frac{\mathcal{G}_I}{\sigma_0} \tag{34.4}$$

where σ_0 refers to the yield strength of the material. The brittle-ductile transition is controlled by a characteristic length scale of material, the plastic radius, $r_p = c\frac{K_{Ic}^2}{\sigma_0^2} = c\frac{E\mathcal{G}_{Ic}}{\sigma_0^2}$, which describes the size of the plastic zone in front of the crack. Here, c is a constant that depends on, for example, the stress state at the crack tip, usually of order 1. Because all materials experience some level of plasticity, in elastoplastic fracture mechanics, d can be directly connected to the magnitude of the J integral. The concept is detailed in Chapter 16 through the following relationship:

$$d = \alpha\frac{J}{\sigma_0} \tag{34.5}$$

with α being the so-called Shih factor of order one, which depends on strain capacity and ratio $\frac{\sigma_0}{E}$. The critical CTOD, d_c, is an alternative fracture toughness indicator equivalent to $J_{Ic} = \mathcal{G}_{Ic} \propto \frac{K_{Ic}^2}{E}$ under small-scale yielding conditions. Both r_p and d_c can be formally related because $\frac{d_c^2}{r_p} \sim \frac{J_{Ic}}{E}$, with the geometric interpretation given in Fig. 34.2. Importantly, the magnitude of d_c offers a mean to quantify what can be considered a sharp crack in the context of fracture mechanics and what can be considered a notch. If the opening of the crack is initially larger than d_c, strictly speaking, the stress concentration cannot be assimilated to a pure crack. In other words, the tip radius of curvature is too low for the tip to be seen as a crack. This means that the maximum opening stress and maximum stress triaxiality ahead of the crack tip are lower than the fracture mechanics level as predicted by the HRR fields [10,11]. Extra energy must thus be dissipated to reinitiate a sharp crack. There are many examples showing that the apparent fracture toughness value indeed increases (and is no longer a true fracture toughness) above a certain threshold set by d_c (or sometimes a value larger than d_c but still connected to it). Thus, the toughening mechanism by blunting is to force the propagating crack to open above the threshold opening (typically d_c), which then arrests the crack and forces a reinitiation. Such "over-opening" can be triggered by forcing the crack to coalesce with cavities or microcracks. One implementation is to have particles with weak bonding to the matrix. As the crack gets very close to the particle, decohesion is created and the crack gets trapped by the void and over-opened. An alternative is to pattern the joint with preexisting open spaces [12–15].

s0030 34.2.3 Crack face bridging

p0050 The principle of toughening via bridging stems from basic fracture energy considerations and aims to increase sources of energy storage and dissipation by additional mechanisms instead of the fracture of bondline materials alone, that is, $\mathcal{G}_c^a$—the fracture energy of the adhesive material [16,17]. The creation of new crack faces in the material experiencing with bridging requires additional energy due to straining of the bridging material and eventual decohesion and/or failure of the ligaments, $\mathcal{G}_c^p$. The bridging phenomena can also equally be regarded as a reduction of the energy release rate; however, the net result remains the same–an increase in measured fracture energy. Thus, in general, the total fracture energy, expressed as $\mathcal{G}_c^T$, can be defined as a sum:

$$\mathcal{G}_c^T = \mathcal{G}_c^a + \mathcal{G}_c^p + \ldots \tag{34.6}$$

where the three dots indicate other dissipation sources that can contribute to the work needed to fracture the joint (Fig. 34.3).

s0035 34.2.4 Architected bondlines and adherends

p0055 Consider a bonded tensile specimen shown in Fig. 34.4A under an applied tensile force P. For simplicity, neglecting any local effects on the stress distribution due

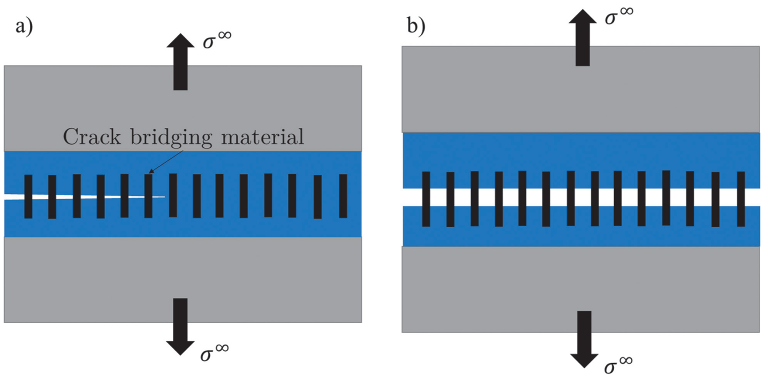

f0020 **Fig. 34.3** Schematic representation of crack bridging phenomena: (A) initial configuration, and (B) after crack propagated through the bondline. In the presented case, under σ^∞ loading, the bridging material extends beyond the d_c of the adhesive material.

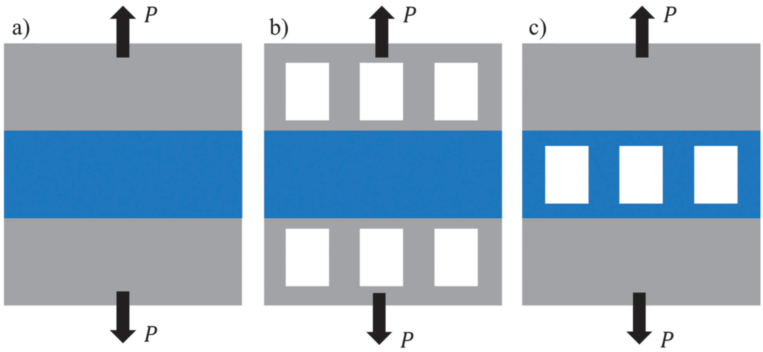

f0025 **Fig. 34.4** Examples of using simple geometrical modifications to control failure loads and stress distribution: (A) reference butt joint; (B) joint with architected adherends; and (C) joint with architected bondline.

to interfaces, edges, or corners, we assume the stress distribution is simply the average stress as given by:

$$\sigma \approx \frac{P}{A_i} = E_i \epsilon_i \tag{34.7}$$

where A_i is the cross-section area, E_i is the Young's modulus, and ϵ_i is the strain. Index i is denoting either the adherend or the adhesive. The stress distribution is affected for the cases depicted in Figs. 34.4B–C because the geometry is spatially varying either in the adherend or in the adhesive domain, respectively. The effect of spatially varying stress can be used to manipulate strain localization, mitigate stresses at the usual failure loci, increase the compliance of the joint, or change the failure modes leading to different mechanical properties of the joint [18].

p0060 On the local scale, the analysis is more involved and we will only make use of fracture mechanics to outline the crucial aspect. Eq. (34.3) gives a simple relationship between the stress field near discontinuities in the plates with a slit and can be rewritten as

$$\sigma(r) \approx \sqrt{\frac{\mathcal{G}_I E}{2\pi r}} \tag{34.8}$$

which can be rearranged to outline the extension of the asymptotic stress field:

$$r \approx \frac{1}{2\pi} \frac{\mathcal{G}_I E}{\sigma^2} \tag{34.9}$$

p0065 For any material with modulus E, there is a material parameter called cohesive length l_c for which $\mathcal{G}_I = \mathcal{G}_{Ic}$ and $\sigma = \sigma_f$ with σ_f denoting the failure stress [19,20]. Consequently,

$$\mathcal{G}_{Ic} \propto \frac{l_c \sigma_f^2}{E} \tag{34.10}$$

p0070 Thus, the fracture energy can be increased by increasing the cohesive length or the failure stress or by decreasing the modulus of the material. Of course, all the parameters are interlinked for homogeneous materials, but the effective E can be independently modified by careful geometrical manipulation. This is the key to architecting the local stress fields through geometry of the adherends and of the bondlines.

s0040 34.3 Embodiments of toughening principles through architecture

s0045 *34.3.1 Stop holes as a crack blunting mechanism*

p0075 As outlined in Section 34.2.2, forcing the crack to reinitiate can be an effective way for increasing fracture toughness of bondlines. Fig. 34.5 shows a realization of this concept through the introduction of holes running through the width of the interface [21].

p0080 Here, so-called "stop holes" are introduced through drilling or molding holes at regular intervals λ along the bondline with diameter D equaling, in the depicted case, that of the adhesive thickness (t_a). The critical parameter, as outlined previously, is D.

s0050 *34.3.2 Alternating surface properties to force bridging and crack meandering*

p0085 New concepts for achieving crack arrest and increased toughness of adhesive joints incorporate patterns for triggering bridging ligaments between the crack faces–resembling fiber bridging phenomena frequently observed in composite delamination. Here, two possible scenarios, shown in Fig. 34.6, have been exploited to improve the effective toughness: (i) bridging through the material embedded in the

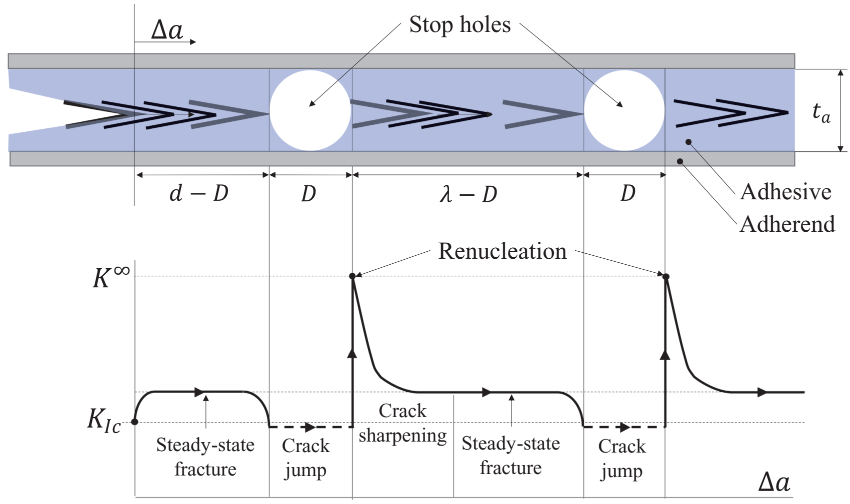

f0030 **Fig. 34.5** Mechanism of toughening by crack blunting using holes with a diameter equal to the adhesive thickness ($t_a = D$). After the period of stable growth through the bondline (region $d - D$), the crack reaches the hole. With no material resistance, the crack jumps over distance D. Here, due to the curvature of the tip being smaller than at the crack tip, the energy required to reinitiate the crack is higher. This process is then repeated.
Adopted from K. Maloney, N. Fleck, Toughening strategies in adhesive joints, Int. J. Solids Struct. 158 (2019) 66–75.

adhesive [22] (Figs. 34.6A–B), and (ii) use of the bondline as the actual bridging ligaments [23] (Fig. 34.6C).

p0090 Both solutions were proven to be successful under mode I loading conditions, leading to a significant increase of bondline fracture energy as well as stabilization of the crack propagation process.

s0055 *34.3.3 Design bondline geometry to control fracture toughness of joints*

p0095 As discussed above in Section 24.2.4, the compliance of the bondline can play a central role in determining how stresses are distributed at the interface and particularly near the crack tip. A more compliant interface results in a larger elastic process zone and reduced stress levels at the crack tip [24]. This approach was implemented in DCB specimens made from PMMA, a model material chosen for its limited ductility (see Fig. 34.7A), structured with pillars at the interface as depicted schematically in Fig. 34.7B.

p0100 The pillar width, d, and spacing, s, of all the specimens were equal and the height of the pillars, t, was varied leading to pillars with aspect ratios (t/d) ranging from 0.5 to 9. The critical failure load of the specimens was a minimum for a pillar with an aspect ratio of 1 and then increased with increasing aspect ratio; see Fig. 34.7C. These trends were observed experimentally and were faithfully predicted by an analytical model

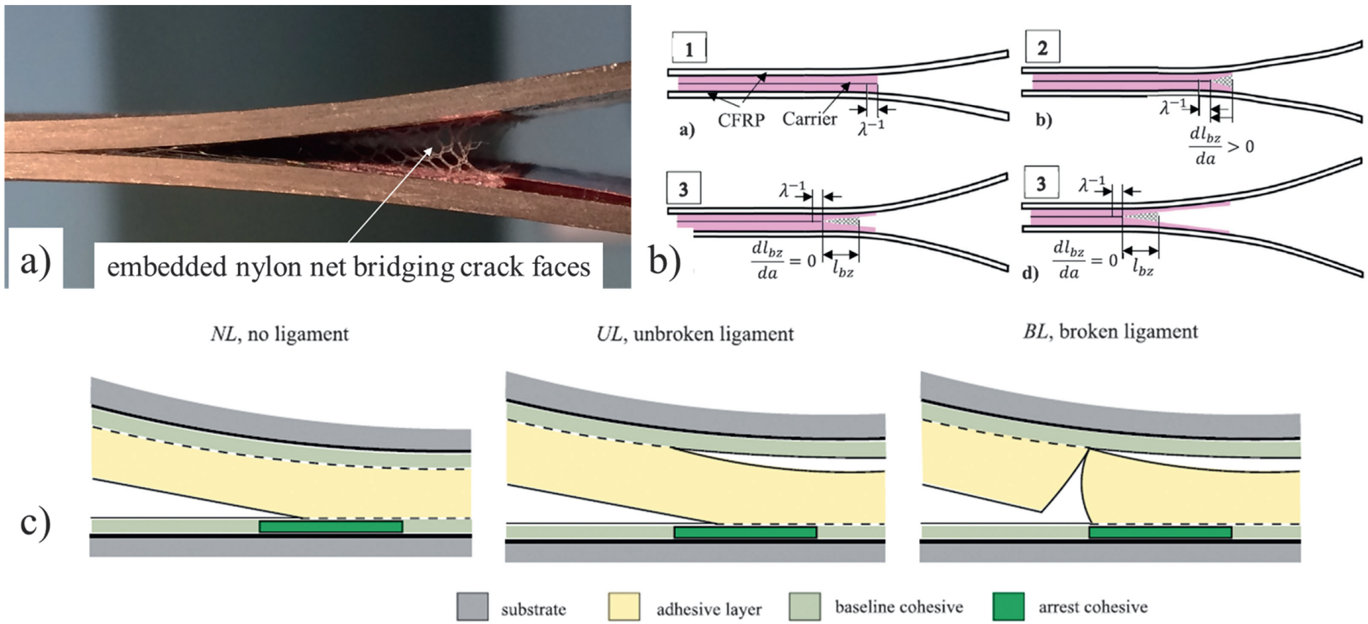

f0035 **Fig. 34.6** Two realizations of toughening through intentional bridging phenomena. (A) Bridging of crack faces through an embedded nylon net with (B) showing the mechanism of fracture process [22]. (C) The mechanism of bridging with the adhesive triggered by designed surface patterning [23].

B978-0-323-91214-3.00012-0, 00012

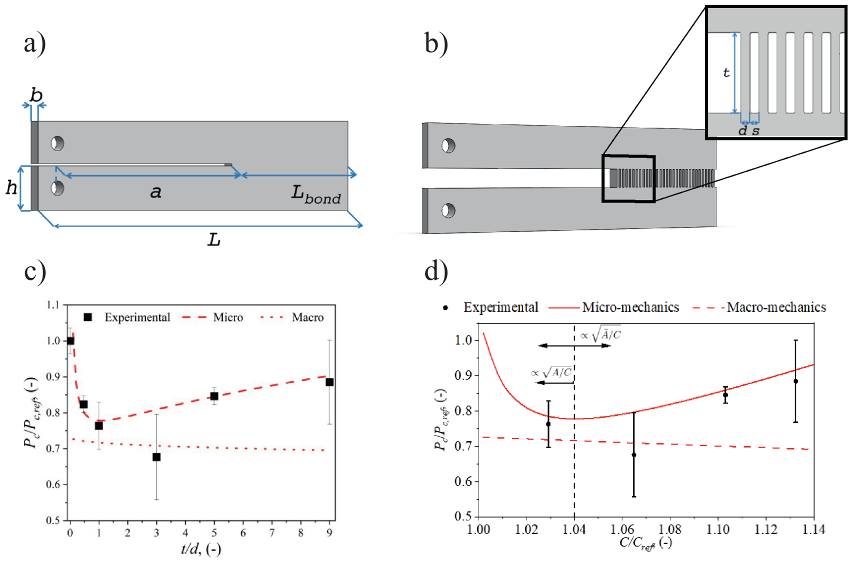

f0040 **Fig. 34.7** Schematic representation of the DCB specimen with: (A) homogeneous bondline of length L_{bond}—the reference configuration, and (B) structured with pillar interface. The details of the architected region are given in the inset. (C) The critical fracture force (normalized with the fracture force of the homogeneous bondline) as a function of the pillar aspect ratio *t*/*d* in the architected region. (D) The normalized fracture force plotted against the normalized specimen compliance. In (C) and (D), model predictions are shown for a "micro" model that predicts failure by considering the failure of a single pillar and a "macro" model that homogenizes the array as a layer of reduced compliance. Only the micro model predicts the experimentally observed behavior.
Based on S. Heide-Jørgensen, M.K. Budzik, K.T. Turner, Mechanics and fracture of structured pillar interfaces, J. Mech. Phys. Solids 137 (2020) 103825.

that combines an elastic foundation and local pillar failure models (i.e., the micro model). The correct behavior was captured by the micromechanics-based theoretical model accounting for pillar geometry while the macroscopic model, based on homogenized properties, and the Winkler foundation model did not match the experimental results. This result shows that brittle adhesives can be toughened using architecture that locally adds compliance; see Fig. 34.7D.

p0105 As the pillar interface is not expected to yield optimal properties for all possible loading directions nor specific failure loads or stiffness, the basic concept can be further exploited. An example of using MM as interfaces was recently reported [25]. MMs are gaining significant attention from both the scientific and industrial communities as an attempt toward rational use of resources, leading to materials with tuned and carefully designed properties obtained by geometrical manipulations of the structure. In the work of Athanasiadis et al. [25], interfaces based on the three different unit cells—pillar, triangular, and hexagonal—were investigated theoretically and numerically; all are depicted in Fig. 34.8A. Using different geometries of the unit cell leads

B978-0-323-91214-3.00012-0, 00012

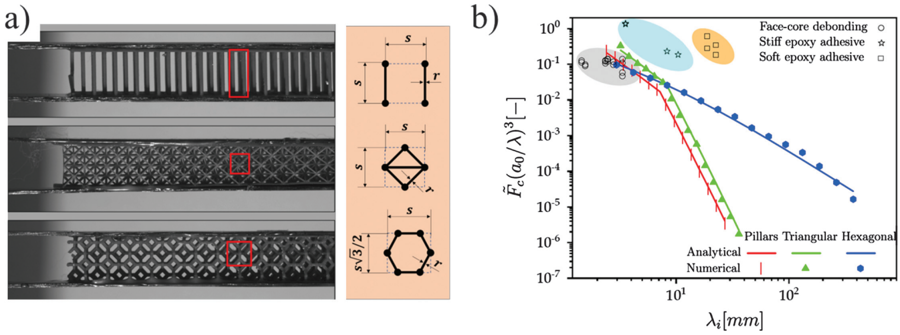

f0045 **Fig. 34.8** (A) Concept of the metamaterial-based interfaces [25] yielding a range of process zone sizes λ_i and leading to a large spectrum of failure loads (B) through manipulating the geometry and size of the unit cell. The typical values used in homogenous systems are also included for reference.

to different sizes of the fracture process zone, λ_i (i standing here for one of the three unit cells), and interface compliances. Noteworthy, λ is a constant for specific joint geometries with homogeneous bondlines. In the case of MM interfaces, it was shown that a full spectrum of λ can be generated by changing the type and dimensions of the unit cell. This in turn results in the range of critical fracture forces; see Fig. 34.8B. Such results open a new design approach in which the bondline will not only join two materials, but can be manipulated to give specific properties, responses under load, or failure modes.

s0060 34.3.4 Designing adherend geometry to control fracture toughness of joints

p0110 Another way of taking advantage of geometry is to exploit it in the design of the adherends. The adherends do not need to have uniform properties, for example the cross-sectional area and/or moment of inertia may vary along the length. The varying cross-sectional area and the second moment of the area introduce variations of the crack tip stress fields, such as extending or reducing the size of the process zone. Such observations were made by Kendall [26] and recently exploited for structural bonding [27]. In the latter study, the DCB specimen was used to evaluate the fracture properties of specimens with different adherend geometries. Contrary to homogenous adherends, the ones used in this study contained bio-inspired voids, circles, and squares with a characteristic dimension d, separated by distance l; see Fig. 34.9A. Depending on the size of the voids and the distance between them, a significant improvement of fracture toughness was achieved. This is shown in Fig. 34.9B, with the inset showing the increase in the work of separation (WOS) as a function of the shape of the void for set values of d and l.

p0115 The adherend geometry can be also used to alter the crack front locus, deflecting the crack from the initial path and changing the local stress components; see Section 34.2.1. The concept of a rectangular zig-zag interface achieved by adherend

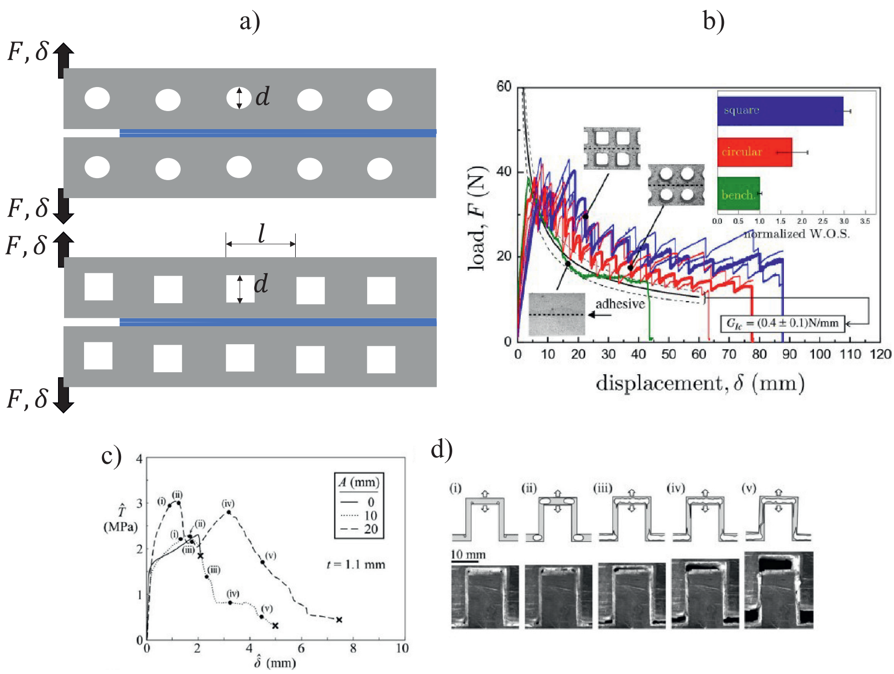

f0050 **Fig. 34.9** Bio-inspired design of adhesive joint fracture through structuring of the adherends [23]: (A) adherend geometries explored, and (B) the resulting force-displacement curves indicating the increase of fracture toughness for specimens with structured adherends. Using adherends to deflect the crack and change local stress components [21]: (C) the average stress vs. displacement curves showing increase of failure loads and work of separation of structured specimens, and (D) the geometry and stages of failure of the joint.

design was exploited by Maloney and Fleck [21]. In Fig. 34.9C, the averaged stress $\widehat{T}$ is reported as a function of applied displacement $\widehat{\delta}$. A significant increase in both the maximum stress and the WOS ($\approx \int \widehat{T} d\widehat{\delta}$) while increasing the adherend overlap distance A is manifested. The geometry relies on converting the globally applied tensile loading into a local stress state at the interface that is mixed mode (mode I and II). Fig. 34.9D shows different stages of joint failure, which are also indicated in Fig. 34.9C. It is observed that after the creation of mode I driven cavities near corners (stage (i) and (ii)), mode I propagation occurs (iii); however, the joint maintains integrity due to the transfer of part of the loading to shear stresses. Eventually, a mode II crack initiates (iv) and propagates (v) until the load-carrying capacity is fully lost.

s0065 *34.3.5 Elastic toughening*

p0120 Elastic heterogeneity along the crack path can be exploited for interface toughening as well. Kendall [26] investigated the peeling of a rubber strip with varying bending rigidity in the peeling direction, as shown in Fig. 34.10A.

B978-0-323-91214-3.00012-0, 00012

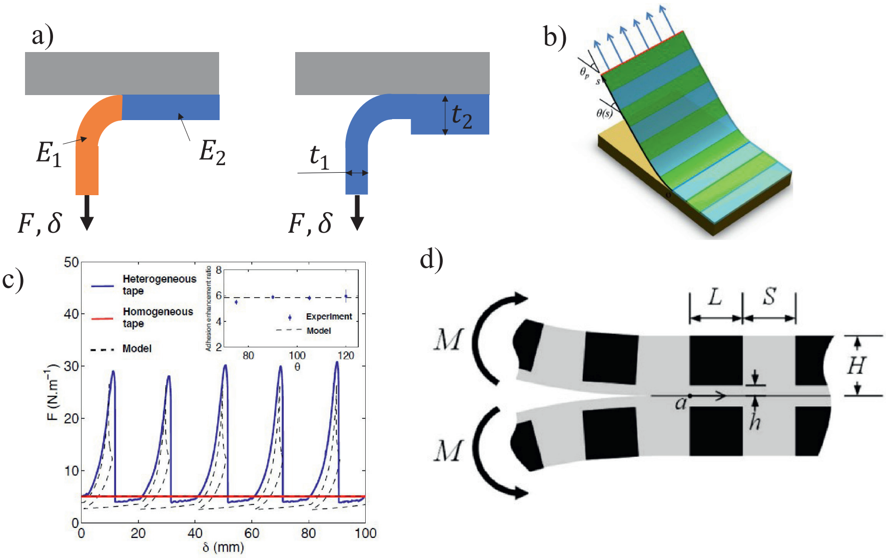

f0055 **Fig. 34.10** Use of elastic toughening principles. (A) Two systems initially investigated by Kendall [26], that is, variation of peeling arm rigidity due to variable modulus and thickness. (B) Materials with periodic stiffness proposed by Xia et al. [28] (C) Effect of varying stiffness on measured peel force compared with the homogeneous stiffness material indicating significant increase of the peeling force despite the same interfacial adhesion properties [28]. (D) A DCB specimen made of material of varying modulus and thickness as analyzed by Luo and Turner [29].

p0125 Kendall found that the crack accelerated when going from a region of high stiffness to a region of low stiffness and slowed when moving from a region of low stiffness to a region of high stiffness. The regions of varying stiffness had a larger peel force than the homogenous case. Xia et al. [28] examined a similar problem of the peeling of a strip with periodic heterogeneity and showed that the peel force increased with local bending rigidity; for example, a factor of eight increase in bending rigidity led to an eight times increase in peel force. Recently, Luo and Turner [29] examined the fracture of DCB specimens with subsurface elastic heterogeneity and demonstrated that similar increases in failure load with increased bending rigidity can be achieved in these geometries, but that the stiff regions must be sufficiently long for the full potential to be realized.

s0070 *34.3.6 Dissipative extra layer*

p0130 In the case in which intrinsic toughening contribution due to plastic dissipation cannot be fully activated, for instance due to the need to use a very stiff specific adhesive with limited plastic dissipation, there is the option to include additional dissipative material layer(s). At least two options have been pursued in the literature, as shown in Fig. 34.11. The first working principle, illustrated in Fig. 34.11A, is simply to intercalate one layer in the stack of adherend and adhesive. When the crack runs in the adhesive sufficiently

B978-0-323-91214-3.00012-0, 00012

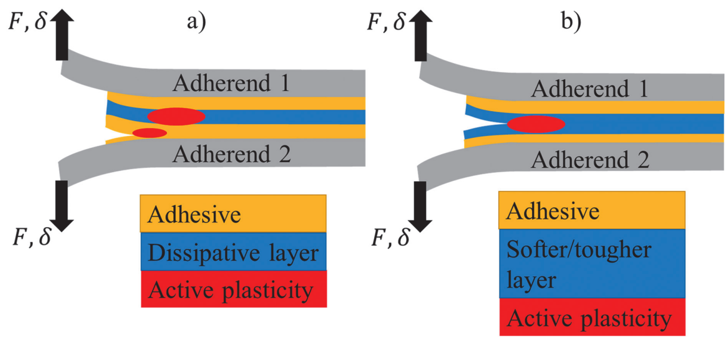

f0060 **Fig. 34.11** Two working principles involving a dissipative interlayer (A) producing extra plastic dissipation while cracking remains inside the adhesive (cohesive, cohesive near the interface, of adhesive), (B) with the crack forced to propagate inside the extra layer being softer than the adhesive.

close to the extra layer, plasticity is induced owing to the large stress carried by the crack and leading to an extrinsic contribution. The second working principle (Fig. 34.11B) is to modify the adhesive layer to favor the presence of a softer but tougher layer that can trap the crack and dissipate more energy. In both cases, the extra layer must be compatible and show good adhesion with the adhesive to avoid premature interface decohesion. These two toughening ways are explained below.

o0010 **(i)** The toughening potential resulting from the introduction of an extra dissipative layer has been recently addressed using the model described in Fig. 34.12A. This is a small-scale yielding model in which the "thin layer" must be seen as the adhesive with thickness h_t [30]. Here, there is no adhesive layer on the other side of the dissipative layer such as in Fig. 34.11A, but the results should essentially be similar. The K field is applied far away from the crack tip region. In this work, the crack was forced to run at the interface between one adherend and the adhesive (adhesive cracking) but the results would not qualitatively change with a cohesive crack within the adhesive layer (= thin layer). The failure process is described by a traction separation law, as shown in Fig. 34.12B, with fracture energy Γ_0 and peak stress σ_c. One set of results considering an elastoplastic interlayer is shown in Fig. 34.12C in terms of the variation of the steady-state toughness Γ_{ss} normalized by Γ_0 as a function of the adhesive bond thickness normalized by the small-scale yielding estimate of the plastic zone size in the absence of interlayer R_0. A very significant effect is observed when h_t/R_0 is small enough compared to the single layer/adhesive system. This analysis has been validated with experiments.

p0140 It is interesting to note in Fig. 34.12C that significant toughening is observed with a purely elastic interlayer as well. The reason is explained in Depinoy et al. [30] and results from additional plasticity in the adhesive layer due to extra bending associated with the deformation of the elastic interlayer. This can be considered another toughening principle associated with the flexible/compliant elastic interlayer.

p0145 This idea of introducing a dissipative interlayer has already been documented before, although not directly in the context of adhesive bonding [31,32]. The work

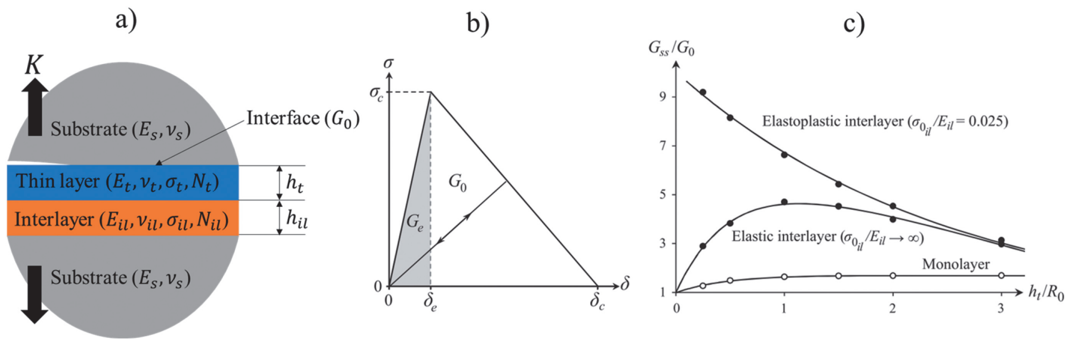

f0065 **Fig. 34.12** The dissipative interlayer concept addressed by a small-scale yielding model with failure process (A) represented through a traction-separation law to provide results regarding increasing the steady-state fracture toughness (B). (C) Variation of the overall interface toughness for the three investigated cases: monolayer alone, elastic interlayer, and plastic interlayer (R_0 is a reference length corresponding to an estimate of the plastic zone size inside the thin layer).

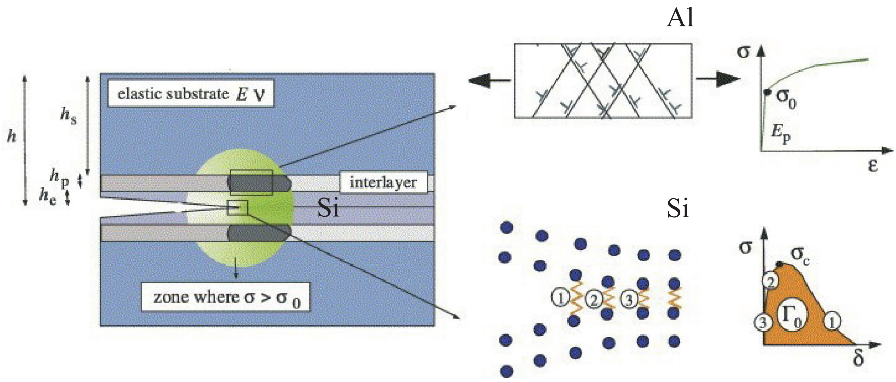

f0070 **Fig. 34.13** Idea of interface toughening of silicon wafer bonding (Bertholet et al. [32]). Silicon (Si) wafers are typically bonded by molecular adhesion between the Si oxide surface layers. The idea was to introduce aluminum (Al) thin dissipative layers intercalated between Si and the Si oxide.

by Bertholet et al. [32] was on silicon wafer bonding. Silicon (Si) wafers are typically bonded by molecular adhesion between the Si oxide surface layers; see Fig. 34.13. The idea was to introduce aluminum (Al) thin dissipative layers intercalated between Si and the Si oxide. Very significant toughening was observed, with an increase of a factor between 2 and 5 due to the plasticity in the Al, as demonstrated experimentally and captured by a cohesive zone-based model. Wei and Hutchinson [31] previously addressed a similar problem from a purely computational viewpoint in the case of a thick dissipative interlayer with similar findings.

o0015 **(ii)** The second option is the introduction of a softer but tougher layer with the crack forced to propagate into the soft layer, as shown in Fig. 34.11B. Even though the layer is tougher, the fact that it is softer leads to a crack trapping effect upon loading. The challenge is to experimentally realize such systems. One option has been recently proposed by Voleppe et al. [33] in which the interlayer is made of thermoplastic PEI, which can be cocured with a thermoset polymer. This research was made in the context of direct epoxy-based composite bonding through a thermoplastic layer. The cocuring process leads to interdiffusion and the creation of a graded layer. The idea is that one of the regions in the gradient is softer but much tougher owing to the presence of PEI. This requires careful control of the curing process to generate the right gradient and is not easily replicated, but the idea is worth pursuing, perhaps with a simpler approach. Ultimately, one could see the perforated bond layer addressed earlier in this chapter as a variant of this idea: the perforated layer is a soft region (due to the cavities) in which the crack is trapped and in which extra toughening is provided through crack arrest and blunting.

s0075 34.4 Summary and possible future trends

p0155 Recent trends in the toughening of adhesive joints through architecture were summarized and discussed. The main issue with architecting adhesive joints is how to avoid the introduction of a new source of damage/embrittlement due to new interfaces. It is

B978-0-323-91214-3.00012-0, 00012

important to appreciate, as shown in the examples treated in this chapter, that fracture toughness includes a length scale and that dissipation will be significant if the volume under consideration is large enough. In other words, architected joints will reach full potential only if they are sufficiently thick. This may lead to important trade-offs concerning property optimization. For instance, for some architectures, the shear stiffness and strength of the joint may decrease significantly, and may impact other structural design constraints. There is thus a need to integrate this joint architecting approach into a wider vision of joint design, including opportunities to make the joints multifunctional.

References

[1] A.J. Kinloch, J.H. Lee, A.C. Taylor, S. Sprenger, C. Eger, D. Egan, Toughening structural adhesives via nano-and micro-phase inclusions, J. Adhes. 79 (8–9) (2003) 867–873.

[2] L. Daelemans, S. van der Heijden, I. De Baere, H. Rahier, W. Van Paepegem, K. De Clerck, Damage-resistant composites using electrospun nanofibers: a multiscale analysis of the toughening mechanisms, ACS Appl. Mater. Interfaces 8 (18) (2016) 11806–11818.

[3] H. Ming-Yuan, J.W. Hutchinson, Crack deflection at an interface between dissimilar elastic materials, Int. J. Solids Struct. 25 (9) (1989) 1053–1067.

[4] H.M. Jensen, Mixed mode interface fracture criteria, Acta Metall. Mater. 38 (12) (1990) 2637–2644.

[5] J.P. Parmigiani, M.D. Thouless, The roles of toughness and cohesive strength on crack deflection at interfaces, J. Mech. Phys. Solids 54 (2) (2006) 266–287.

[6] F.A. Cordisco, P.D. Zavattieri, L.G. Hector Jr., B.E. Carlson, Mode I fracture along adhesively bonded sinusoidal interfaces, Int. J. Solids Struct. 83 (2016) 45–64.

[7] D. Martinez, V. Gupta, Energy criterion for crack deflection at an interface between two orthotropic media, J. Mech. Phys. Solids 42 (8) (1994) 1247–1271.

[8] E. Martin, D. Leguillon, C. Lacroix, A revisited criterion for crack deflection at an interface in a brittle bimaterial, Compos. Sci. Technol. 61 (12) (2001) 1671–1679.

[9] M. Alam, J.P. Parmigiani, J.J. Kruzic, An experimental assessment of methods to predict crack deflection at an interface, Eng. Fract. Mech. 181 (2017) 116–129.

[10] T. Ikeda, A. Yamashita, D. Lee, N. Miyazaki, Failure of a ductile adhesive layer constrained by hard adherends, J. Eng. Mater. Technol. 122 (1) (2000) 80–85.

[11] K.M. Liechti, E.C. Hanson, Nonlinear effects in mixed-mode interfacial delaminations, Int. J. Fract. 36 (3) (1988) 199–217.

[12] S.R. Ranade, Y. Guan, R.B. Moore, J.G. Dillard, R.C. Batra, D.A. Dillard, Characterizing fracture performance and the interaction of propagating cracks with locally weakened interfaces in adhesive joints, Int. J. Adhes. Adhes. 82 (2018) 196–205.

[13] C. Cuminatto, G. Parry, M. Braccini, A model for patterned interfaces debonding—application to adhesion tests, Int. J. Solids Struct. 75 (2015) 122–133.

[14] S. Heide-Jørgensen, M.K. Budzik, Effects of bondline discontinuity during growth of interface cracks including stability and kinetic considerations, J. Mech. Phys. Solids 117 (2018) 1–21.

[15] A. Pascuzzo, A. Yudhanto, M. Alfano, G. Lubineau, On the effect of interfacial patterns on energy dissipation in plastically deforming adhesive bonded ductile sheets, Int. J. Solids Struct. 198 (2020) 31–40.

[16] C.H. Wang, L.R.F. Rose, A crack bridging model for bonded plates subjected to tension and bending, Int. J. Solids Struct. 36 (13) (1999) 1985–2014.

[17] M. Perelmuter, Analysis of interaction of bridged cracks and weak interfaces, Int. J. Mech. Sci. 149 (2018) 349–360.
[18] S. Kumar, B.L. Wardle, M.F. Arif, J. Ubaid, Stress reduction of 3D printed compliance-tailored multilayers, Adv. Eng. Mater. 20 (1) (2018) 1700883.
[19] A. Hillerborg, M. Modéer, P.E. Petersson, Analysis of crack formation and crack growth in concrete by means of fracture mechanics and finite elements, Cem. Concr. Res. 6 (6) (1976) 773–781.
[20] R.B. Sills, M.D. Thouless, Cohesive-length scales for damage and toughening mechanisms, Int. J. Solids Struct. 55 (2015) 32–43.
[21] K. Maloney, N. Fleck, Toughening strategies in adhesive joints, Int. J. Solids Struct. 158 (2019) 66–75.
[22] S. Heide-Jørgensen, S.T. de Freitas, M.K. Budzik, On the fracture behaviour of CFRP bonded joints under mode I loading: effect of supporting carrier and interface contamination, Compos. Sci. Technol. 160 (2018) 97–110.
[23] R. Tao, X. Li, A. Yudhanto, M. Alfano, G. Lubineau, On controlling interfacial heterogeneity to trigger bridging in secondary bonded composite joints: an efficient strategy to introduce crack-arrest features, Compos. Sci. Technol. 188 (2020), 107964.
[24] S. Heide-Jørgensen, M.K. Budzik, K.T. Turner, Mechanics and fracture of structured pillar interfaces, J. Mech. Phys. Solids 137 (2020), 103825.
[25] A.E. Athanasiadis, M.A. Dias, M.K. Budzik, Can confined mechanical metamaterials replace adhesives? Extreme Mech. Lett. 48 (2021), 101411.
[26] K. Kendall, Control of cracks by interfaces in composites, Proc. R. Soc. Lond. A Math. Phys. Sci. 341 (1627) (1975) 409–428.
[27] A. Wagih, R. Tao, G. Lubineau, Bio-inspired adhesive joint with improved interlaminar fracture toughness, Compos. A: Appl. Sci. Manuf. 149 (2021), 106530.
[28] S. Xia, L. Ponson, G. Ravichandran, K. Bhattacharya, Toughening and asymmetry in peeling of heterogeneous adhesives, Phys. Rev. Lett. 108 (19) (2012), 196101.
[29] A. Luo, K.T. Turner, Adhesion of beams with subsurface elastic heterogeneity, J. Mech. Phys. Solids 159 (2022), 104713.
[30] S. Depinoy, F. Strepenne, T.J. Massart, S. Godet, T. Pardoen, Interface toughening in multilayered systems through compliant dissipative interlayers, J. Mech. Phys. Solids 130 (2019) 1–20.
[31] Y. Wei, J.W. Hutchinson, Models of interface separation accompanied by plastic dissipation at multiple scales, Int. J. Fract. 95 (1) (1999) 1–17.
[32] Y. Bertholet, B. Olbrechts, B. Lejeune, J.P. Raskin, T. Pardoen, Molecular bonding aided by dissipative inter-layers, Acta Mater. 55 (2) (2007) 473–479.
[33] Q. Voleppe, W. Ballout, P. Van Velthem, C. Bailly, T. Pardoen, Enhanced fracture resistance of thermoset/thermoplastic interfaces through crack trapping in a morphology gradient, Polymer 218 (2021), 123497.

Non-Print Items

Abstract

In this chapter, strategies for improving the properties of adhesive joints through geometry and internal structuring are presented, with a focus on recent developments. In the past several years, multiple approaches have been explored to use architecture, patterning, and material heterogeneity to enhance the toughness and damage tolerance of adhesive joints. Many of these strategies exploit well-known phenomena such as crack front deflection, crack blunting, and the introduction of dissipative and/or bridging layers. The objective of this chapter is to review several principles that can be used to enhance toughness as well as show several embodiments of these principles through architecting of joints.

Keywords: Architected joints, Crack face bridging, Crack deflection, Crack tip blunting, Surface Patterning, Dissipative layers.